Journal of Luminescence 30 (1985) 520–540
North-Holland, Amsterdam

EXCITONS IN GaAs QUANTUM WELLS

R.C. MILLER and D.A. KLEINMAN

AT&T Bell Laboratories, Murray Hill, New Jersey, 07974, USA

This paper attempts to summarize some of the salient properties of excitons in GaAs quantum wells and in doing so it will emphasize work at AT&T Bell Labs with which the authors have been associated. Although the text relies heavily on published material, an effort has been made to stress new material, and where feasible, unpublished aspects, e.g., figures, related to earlier work. Topics discussed on the quasi-2D excitons in GaAs quantum wells include: their inherent tendency for intrinsic free-exciton emission, exciton binding energies, bound and localized excitons including biexcitons and excitons bound to neutral impurities, effects of n- and p-type modulation and antimodulation doping, and the developments leading to a proposed set of quantum well parameters that results in acceptable fits to the observed exciton transitions for GaAs quantum wells with both square and parabolic potential profiles.

1. Introduction

It was evident from the earliest work by Dingle et al. [1] on the optical properties of GaAs quantum wells grown by molecular beam epitaxy (MBE) with the GaAs–AlGaAs system that excitons play a much more significant role in these quasi-2D systems than in bulk GaAs. The photoluminescence at low temperatures from a few microns of high-quality MBE-grown undoped GaAs is usually characterized by emission at ≈ 1.49 eV due to donor–acceptor pair recombination (D^0–A^0) and free electron–neutral acceptor recombination (e–A^0) plus emission at the exciton edge, $\cong 1.515$ eV, due mainly to excitons bound to D^0 and A^0, and hole–neutral donor (h–D^0) recombination. Small contributions due to free-exciton (polariton) emission are also frequently observed. However, the main point is that for the bulk GaAs grown by MBE the emission at low excitation levels is usually predominantly extrinsic in nature [2].

This is in marked contrast to GaAs quantum wells with similar purity to the bulk GaAs material mentioned above. Absorption, emission, and excitation spectra of high-quality GaAs quantum wells with good interfaces demonstrate that intrinsic free-exciton recombination dominates the emission even at very

0022-2313/85/$03.30

low temperatures where bound exciton and impurity processes dominate for the bulk GaAs [2,3].

Extensive absorption spectra obtained by Dingle et al. [1,4] on multiquantum well samples from which the GaAs substrate had been etched off (window samples) revealed sharp peaks at the onset of the band to band transitions showing that exciton effects are also pronounced in absorption. A classic example of this is shown in fig. 12 of ref. [4]. In the absence of such exciton effects, the onset of the various band-to-band transitions should be step-like reflecting the step-like changes in the 2D density-of-states. Excitation spectra taken later also lead to the same conclusions [3,5].

The splitting of the heavy and light hole bands in GaAs quantum wells due to their different effective masses leads to well resolved heavy and light hole exciton transitions in absorption [4] and emission [3,5]. The assignments of these transitions were made initially on the basis of the good agreement between the observed and calculated transition energies. However, linear and circular optical polarization measurements provided direct confirmation of these light and heavy hole assignments [3,5].

Since optical electron spin orientation using circular polarization excitation and detection techniques [6] will be mentioned frequently throughout this paper, some of the underlying principles will be discussed briefly with the aid of fig. 1(b). The relevant circular polarization phenomena are determined by the relative transition strengths (3 and 1), the m_j values ($\pm 3/2$ and $\pm 1/2$), and the effective hole masses $m_h^* = 0.45 m_0$ [7] and $m_l^* = 0.088 m_0$ [8] for the heavy and light holes, respectively. The absorption and emission processes considered are for detection and excitation at normal incidence to the plane of the layers. Since the electron states are $m_j = \pm 1/2$, the resonant absorption of $\sigma^+ (\Delta m_j = +1)$ polarized light by heavy and light hole transitions will generate electrons with $m_j = -1/2$ and $+1/2$, respectively. With $m_h^* > m_l^*$, the emission at low temperatures will be via the heavy hole ground state. Thus assuming a spin relaxed hole population [9] and incomplete electron spin relaxation, resonant excitation of the lowest energy heavy or light hole exciton transitions should lead to emission from the ground-state heavy hole exciton polarized σ^+ and σ^-, respectively. Likewise, at elevated temperatures where the lowest light hole level is thermally populated, the above resonant excitation conditions should give rise to emission from the ground-state light hole exciton with polarization σ^- and σ^+, respectively. As there is always some relaxation of the electron spins, the luminescence is never 100% polarized. In any event, a decreased, or a negative polarization, i.e., a polarization opposite to the incident polarization, is the hallmark of light hole transitions in excitation with detection set at the heavy hole emission which is the usual way of obtaining an excitation spectrum. For nonresonant excitation, σ^+ emission at low temperatures dominates since the heavy hole transitions are 3 times the strength of the light hole transitions. Thus circular polarization techniques can be very useful in identifying transitions

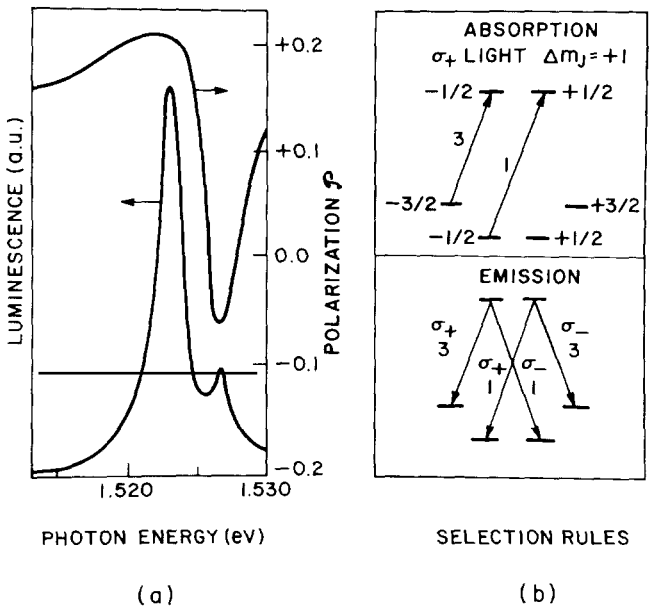

Fig. 1. (a) Photoluminescence and its circular polarization at 50 K for excitation at 1.65 eV with circular polarized light. The sample has 25 GaAs wells with $L = 188$ Å and 19 Å $x = 0.3$ alloy barriers. For this nonresonant excitation, $m_j = -1/2$ electron states are preferentially created which leads to heavy and light hole exciton emission with positive and negative polarizations, respectively. (b) Absorption and emission transitions for GaAs quantum wells with circular polarized light. The transitions involving heavy ($m_j = \pm 3/2$) and light ($m_j = \pm 1/2$) holes have relative strengths of 3 and 1, respectively.

(fig. 1(a)) and indeed have been utilized to verify the original assignments by Dingle et al. [3,5]. Although not discussed herein, the decrease in polarization of the emission with a transverse magnetic field (Hanle effect) can be used to estimate the electron lifetime and the electron spin relaxation time [5,6].

The intrinsic free-exciton nature of the recombination mentioned above for GaAs quantum wells is deduced largely from the observed small Stokes shift (a fraction of the line width) between the heavy hole photoluminescence emission and the heavy hole ground-state exciton absorption peak [3,5]. Likewise, when the photoluminescence emission investigated involves the light hole, there is at most a small Stokes shift between emission and absorption. Weak extrinsic photoluminescence is frequently observed from undoped GaAs quantum wells of the same quality as that mentioned above [10]. The most easily identified extrinsic emission has been that due to e A^0 where carbon is thought to be the neutral acceptor.

2. Exciton binding energies

Dingle et al. [1,4] were able to estimate the binding energy of the quasi-2D excitons for GaAs quantum wells of width L by extrapolating to zero the confinement energies of the various exciton peaks measured in absorption. In this manner, the exciton binding energy was estimated to be ≈ 9 meV for $L \lesssim 100$ Å. This is to be compared with 4.2 meV for bulk GaAs. However, a number of GaAs quantum well samples showed explicit structure in the excitation spectrum which could be identified with excited and/or continuum states of the 2D excitons. One of the best examples of this is shown in fig. 2 which gives the excitation spectrum for an unusually good single well sample with $L = 50$ Å and alloy barriers of width $L_b = 0.65\,\mu$m with $x = 0.37$. Throughout this work, allowed transitions involving electrons and holes of quantum number n, where $n = 1, 2, 3$, etc. with $\Delta n = 0$, will be identified by E_{ni} where $i = h$ for heavy holes and ℓ for light holes. Forbidden transitions where $\Delta n \neq 0$ will be identified by E_{ijk} where i is the electron quantum number, j the hole quantum number, and k the type of hole, either h or ℓ. Thus the parity allowed $\Delta n = 2$ transition between the $n = 1$ electron and $n = 3$ heavy hole is designated $E_{1\,3h}$.

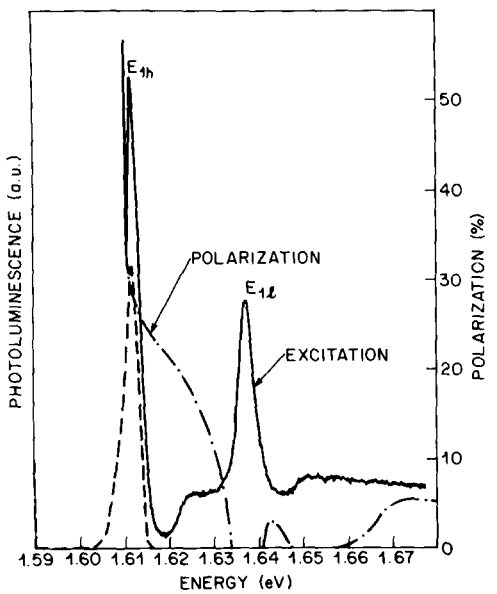

Fig. 2. Photoluminescence (dashed), excitation (solid) and smoothed polarization (dashed dot) spectra at 5 K for a single GaAs well sample with $L = 50$ Å. For the excitation spectrum detection was at 1.611 eV. The polarization actually goes negative in the 1.637 eV and 1.652 eV spectral regions. The data show that the shoulders in the photoluminescence at 1.624 eV and 1.652 eV are heavy and light hole character, respectively. It is proposed that these shoulders represent the onset of excited exciton states.

Of most interest in fig. 2 are the distinct shoulders on the high-energy side of the E_{1h} and $E_{1\ell}$ exciton peaks which the polarization shows are heavy and light hole character, respectively. It is concluded that these shoulders represent the onset of heavy and light hole excited states and that the discrete excited states in this case are not resolved from the continuum. Also it should be noted that the luminescence level at the light hole continuum edge is about 4/3 that at the heavy hole continuum edge which is consistent with heavy and light hole band relative strengths of 3 and 1, respectively. The apparent continuum edge is taken to be the 2S excited state of the exciton. In this interpretation the true continuum edge corresponding to the ionization threshold is not seen directly in these spectra. The midpoint of the rising portion of the shoulder is taken as the 2S level while the 1S level is the exciton peak itself. This therefore provides a direct measurement of the term value $B_{1S}-B_{2S}$. Since the in-plane heavy hole mass is less than that of the light hole, the binding energy of the light hole exciton is expected to be greater than that of the heavy hole exciton as is observed [11]. Similar results have been obtained in the same manner for samples with L ranging 42 Å to 340 Å. However for $L=340$ Å, a distinct peak in the excitation spectrum is attributed to the 2S heavy hole exciton excited state. The term values B_{1S} B_{2S} increase with decreasing L and for example, for $L=50$ Å (fig. 2), $B_{1S}(\ell)$ $B_{2S}(\ell)=10.7$ meV.

These data have been compared with a variational calculation of the exciton binding B_{1S} and the term value $B_{1S}-B_{2S}$ as a function of L for GaAs quantum wells with infinite potential barriers [11]. The formulation contains no adjustable parameters other than the variational parameter and it is exact for $L\to 0$. Since the calculated term values are found to be in good agreement with the data, the calculated B_{1S} values can be considered reliable. It is interesting to note that the 9 meV value for B_{1S}(h) estimated by Dingle et al. [4] is in good agreement with these results. The integrated strengths of the light and heavy hole excitons were also calculated and found to be in reasonable agreement with the data where the continuum thresholds were sufficiently well resolved [11]. The calculated strength increases by about a factor of 2 as L decreases from 140 Å to 42 Å.

This calculation [11], and a subsequent one by Bastard [12], assume no penetration into the alloy barriers, i.e., infinitely high potential wells. Greene et al. [13] have taken finite barriers into account and show that, as expected, the B_{1S} values are reduced for small L due to penetration. As a result, the B_{1S} values from Greene et al. for small L are somewhat less than those determined with no penetration and hence lead to $B_{1S}-B_{2S}$ term values somewhat less than the data as interpreted in ref. [11]. Also Greene et al. find that the effects due to penetration for the light hole exciton are sufficiently more pronounced than those for the heavy hole exciton to give $B_{1S}(\ell)<B_{1S}$(h) for $L<50$ Å and $x=0.3$ alloy barriers. The data in fig. 2 for $L=50$ Å and $x=0.37$ alloy barriers, suggest that $B_{1S}(\ell)>B_{1S}$(h).

3. Bound and localized excitons

3.1. Biexcitons

Biexcitons are perhaps the simplest form of bound excitons and there are data that suggest that this species does indeed exist at low temperatures (≈ 5 K) in high-quality GaAs quantum wells [14]. Samples grown under conditions which lead to intense, sharp, photoluminescence peaks, and excitation spectra which indicate abrupt interfaces and wells of uniform thicknesses usually exhibit a luminescence peak in the region of the free exciton which consists of two sharp components. An example of this is shown in fig. 3. At the lowest excitation intensities, $I_p \approx 1$ mW cm^{-2}, one peak is observed which excitation spectra show is due to the E_{1h} free exciton. As I_p is increased, a shoulder appears on the low-energy side, and finally at sufficiently high I_p, two distinct peaks separated by ≈ 1 meV are observed. The splitting and the energy of the E_{1h} peak are independent of I_p. When T is increased to ≈ 11 K, $kT \approx 1$ meV, the free-exciton peak always dominates and its intensity is enhanced. This temperature dependence was observed for all samples which exhibited the two sharp

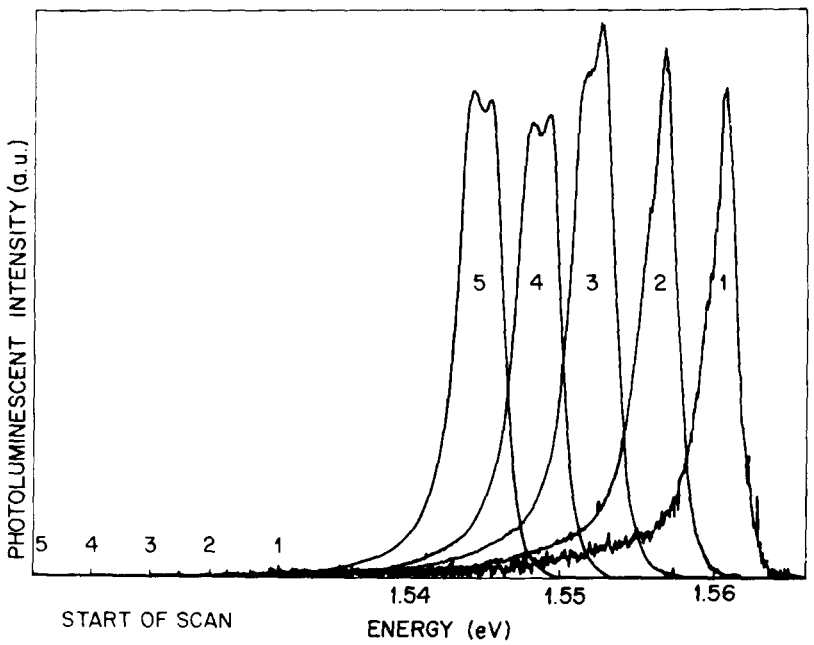

Fig. 3. Photoluminescent intensity at 5 K from a sample with 81 Å GaAs quantum wells and 200 Å $x=0.26$ alloy barriers versus emission energy for excitation at 1.695 eV with 1.4 mW/cm^2 (1), 3.1 mW/cm^2 (2), 21.2 mW/cm^2 (3), 45.3 mW/cm^2 (4), and 187 mW/cm^2 (5). The peak at lower energy attributed to biexcitons comes in clearly at about 20 mW/cm^2.

peaks. Also, the change from one peak to two peaks with increasing I_p was observed with samples where L ranged from 81 Å to 327 Å. The "threshold" I_p for the second peak tends to decrease with increasing L, and two samples with $L > 327$ Å exhibited two peaks even at the lowest intensities, ≈ 1 mW/cm^2.

With excitation by polarized light, a pronounced minimum in the polarization at the lower-energy peak has been observed [14]. This observation is consistent with zero polarization for the process responsible for this peak. If this peak is indeed due to biexcitons as proposed, it would be expected to radiate with zero polarization. However the fact that this distinct minimum in the polarization is not always observed was tentatively attributed to the need for a detailed line-shape analysis.

Thus, the dependence of the lower-energy peak on excitation intensity, temperature, and polarization is consistent with a 2D biexciton with a binding energy of ≈ 1 meV. Kleinman [15] has made a variational calculation of the binding energy B_{xx} of the biexciton in GaAs quantum wells. This calculation contains no adjustable parameters other than the variational parameters and makes use of the six-parameter wavefunction of Brinkman, Rice, and Bell which yields $B_{xx} = 0.13$ meV for bulk GaAs [16]. For GaAs quantum wells it is found that the calculated biexciton binding energy obeys Haynes's rule [17] with a Haynes constant $f_H \cong 0.1$, i.e., $B_{xx} \cong 0.1 B_{1S}(h)$, and that in the 2D limit B_{xx}/B_{1S} is 3–4 times larger than the corresponding quantity in the 3D case. The calculated values of B_{xx} are in good agreement with the ≈ 1 meV splittings mentioned above for $L < 250$ Å. However for $L > 250$ Å, the observed splittings are too large, suggesting as noted below, that some other mechanism might be relevant for this range of L.

3.2. Excitons bound to neutral donors

Kleinman has also estimated the binding energy B_{XD} of excitons bound to neutral donors for the GaAs quantum well 2D system [15]. These values are larger than B_{xx} and are also found to obey Haynes's rule with $f_H \cong 0.1$ as above for biexcitons. For $L > 250$ Å the observed splittings discussed above tend to agree with the calculated B_{XD} but this agreement should be viewed with caution since the development of this "biexciton" peak with increasing I_p is not expected for excitons on neutral centers.

3.3. Excitons bound to neutral acceptors

A photoluminescence peak attributed to ground-state E_{1h} excitons bound to neutral acceptors (E_{1h}–A^0) has been observed from GaAs quantum wells doped with [Be] $\approx 10^{17}$ cm^{-3} or zinc diffused [18]. Both single and multiple quantum wells have exhibited this extrinsic luminescence. In the four cases where this

luminescence peak has been reported the wells were p-type doped, free E_{1h} excitons were in evidence, the luminescence peak exhibited evidence of saturation, and it decreased rapidly in intensity with increasing T. Also the Stokes shift of this peak from E_{1h} was too small to be attributed to $e-A^0$ recombination which in fact could be identified as additional structure in the photoluminescence. The dissociation energy E_d of the $E_{1h}-A^0$ complex into A^0 and a free E_{1h} exciton was obtained directly from the observed separation of this extrinsic peak from the intrinsic E_{1h} peak. For GaAs quantum wells with $L=46$ Å, $E_d=6.5$ meV. It was noted that E_d decreases with increasing L obeying Haynes's rule with $f_H \approx 0.13$. No convincing evidence of this $E_{1h}-A^0$ emission had been seen in the 100 or so undoped GaAs quantum well samples examined. The photoluminescence from two quantum well structures similar to the Be-doped ones mentioned above but with $[Be] = \approx 3\times10^{16}\,cm^{-3}$ exhibited two $e-Be^0$ peaks, a strong E_{1h} peak, but no discernible $E_{1h}-Be^0$ recombination peak. Thus in contrast to bulk GaAs, $[Be] \cong 10^{17}\,cm^{-3}$ would seem to be required with the GaAs quantum wells studied to produce an easily observed $E_{1h}-Be^0$ luminescence. This is regarded as evidence that E_{1h} excitons in GaAs quantum wells do not migrate easily so that only when the average separation of the Be^0 centers is comparable to the exciton diameter $\cong 300$ Å [11] will this emission be observed.

3.4. Excitons localized by weak disorder

The exciton transition at low temperature in relatively pure high quality GaAs quantum wells often exhibits a strong resonant Rayleigh scattering [19]. When the incident laser frequency is well outside the exciton resonance a weak Rayleigh scattering is observed due to defect scattering. When it is close to the resonance the Rayleigh scattering increases by as much as 200 times the defect scattering. The scattering has the same spectral and temporal profile as the laser light, and therefore can be distinguished from the ordinary luminescence. Hegarty et al. [19], have attributed this scattering to spatial fluctuations of the exciton resonance frequency due to fluctuations of the effective well width L. We note that fluctuations in L which are multiples of half the lattice constant can arise from a step-like growth during MBE, while smaller fluctuations with a continuous distribution (weak disorder) may arise from random concentration fluctuations of Al in the barriers. On the basis of an assumed Lorentzian model for the exciton line shape, Hegarty et al. [19] have analyzed the absorption and resonant Rayleigh scattering spectra of several samples to obtain the frequency variation of the homogeneous width across the exciton line. The results show that the broadening is inhomogeneous on the low-frequency side of the absorption peak, but the homogeneous contribution rises (and the inhomogeneous contribution falls) rapidly with increasing frequency near the absorption peak. Also the homogeneous part increases with increasing temperature. These

results are consistent with the following picture of the free-exciton transition: (a) the energy spectrum is continuous, but due to the weak disorder there exists a "mobility edge" near the absorption peak separating localized states below the edge from delocalized states above the edge; (b) below the edge the line shape (inhomogeneously broadened) represents the density of localized states; (c) above the edge the line shape (homogeneously broadened) represents the scattering of freely migrating excitons by the weak disorder.

4. Excitons in modulation doped GaAs quantum wells

It is to be expected that quasi-2D electron or hole gases in sufficient concentration in GaAs quantum wells will affect the exciton characteristics of these structures. Some interesting effects on the quantum-well excitons believed due to charge carriers was noted during studies of single GaAs quantum wells grown by metalorganic chemical vapor deposition (MOCVD) [20]. While the better samples grown by MOCVD were comparable exciton-wise to the best MBE-grown material, many exhibited an anomalous excitation spectrum. In particular, the E_{1i} transitions were weakened compared to E_{2h}, especially E_{1h}, all exciton peaks were broadened, the emission was Stokes shifted from E_{1h}, and the photoluminescence increased gradually as the excitation photon energy E_p approached $E_{1\ell}$ from the high-energy side. In some cases, as shown in fig. 4, the E_{1h} transition was missing altogether while the other exciton transitions including $E_{1\ell}$ were very much in evidence. Furthermore as T was increased from 5 K to 77 K a distinct peak due to E_{1h} appeared in the excitation spectrum near the expected energy. These observations led to the speculation the anomalous behavior may be due to holes in the GaAs quantum wells [20].

4.1. p-type modulation doped quantum wells

Of much interest from a device as well as a physics point of view are the "modulation doped" structures in which the n- or p-type dopants are restricted during growth to the alloy barriers [21]. In order to maintain a constant Fermi level in such a quantum well structure, the dopants in the alloy barriers ionize with the free carriers migrating to the lower-energy undoped quantum wells. Thus one has a situation where the ionized impurities are spatially separated from the carriers and the resultant carrier mobilities high [21].

Figure 5 shows the photoluminescence spectra for a p-type modulation doped sample grown by MBE with 20 periods of $L = 115$ Å GaAs wells and 150 Å $x = 0.44$ alloy barriers. The middle 50 Å of each barrier was doped with [Be] $\approx 10^{18}$ cm^{-3} which led to a 2D-concentration $N_h = 5.4 \times 10^{10}$ cm^{-2} at 5 K. The excitation spectrum for this sample is anomalous in the same sense as

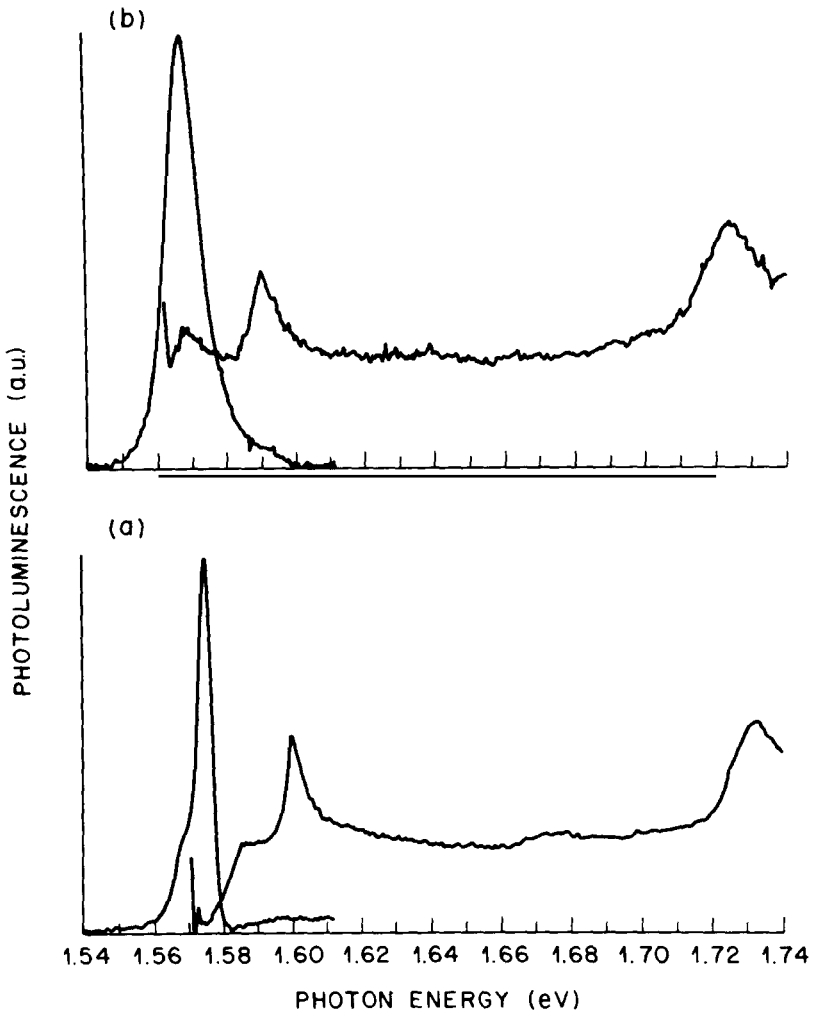

Fig. 4. Photoluminescence and excitation spectra from a single GaAs quantum well with $L = 70$ Å grown by metalorganic chemical vapor deposition. In (a) at 6 K, the E_{1h} peak is missing while $E_{1\ell}$ (1.60 eV) and E_{2h} (1.73 eV) are clearly seen in the excitation spectrum. At 77 K (b) a peak attributed to E_{1h} appears (1.567 eV) and is shifted from the free exciton emission peak by $\cong 1$ meV. The detector gain in (b) is four times that of (a).

described above for the MOCVD single-well samples. Such characteristics have been observed with other Be-modulation doped multiquantum well samples with $N_h \approx 10^{11}$ cm^{-2}.

Another sample also grown by MBE had 20 periods of $L = 90$ Å GaAs wells and 550 Å $x = 0.45$ alloy barriers with the center 43 Å of each doped with Be =

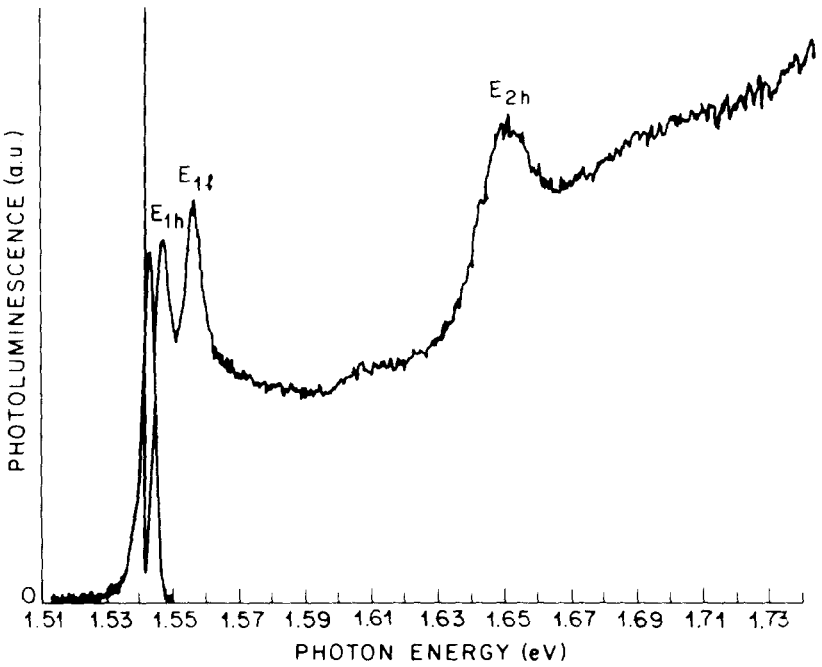

Fig. 5. Photoluminescence and excitation spectra at 5 K for a p-type modulation doped multi-quantum well sample with 115 Å wells and 150 Å $x=0.44$ alloy barriers. The low-temperature 2D carrier density is $N_h = 5.4 \times 10^{10}$ cm^{-2}. The main effects on the excitons due to the holes are in the region of E_{1h} and $E_{1\ell}$ as discussed in the text.

2×10^{18} cm^{-3} to yield $N_h = 5.3 \times 10^{11}$ cm^{-2} at low temperatures. In this case, as shown in fig. 6, at 5 K the E_{1h} transition is missing and the circular polarization shows that the lowest energy peak is light hole in character. However, as T is increased a shoulder appears on the low-energy side of the peak assigned to $E_{1\ell}$ and finally at 43 K a distinct peak due to E_{1h} is seen as shown in fig. 7. There is a sizeable Stokes shift between the emission and the absorption peak due to E_{1h} contributions.

It is most interesting that the E_{1h} exciton peak can be completely absent from the excitation spectrum at low temperatures while other excitons, both light ($E_{1\ell}$) and heavy excitons (E_{2h}), still retain significant strength. The absence of E_{1h} at low temperatures and its reappearance as T is increased has been observed for a number of different samples and for N_h as low as $\approx 3 \times 10^{11}$ cm^{-2}. Screening of the excitons by the holes would seem to be ruled out since screening should affect all excitons in roughly the same manner which is clearly not the case. It has been suggested [22] that at low temperatures heavy hole band filling prevents the formation of E_{1h} excitons due to the Pauli exclusion principle, i.e., the hole states required to form excitons are already filled. Then as the

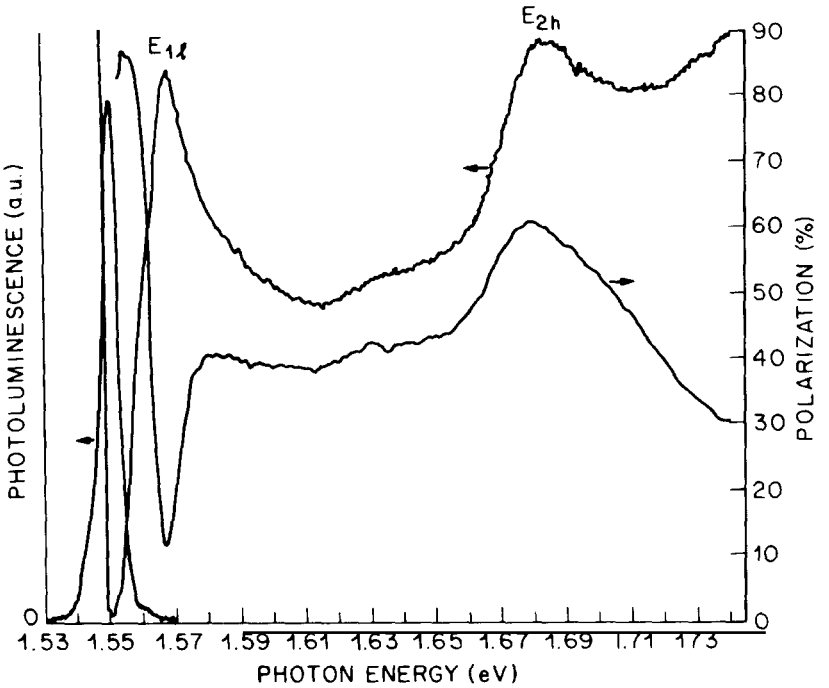

Fig. 6. Photoluminescence, excitation, and polarization spectra at 5 K for p-type modulation doped multiquantum well sample with 90 Å wells and 550 Å $x=0.45$ alloy barriers with the center 43 Å doped to give $N_h = 5.3 \times 10^{11}$ cm^{-2}. The exciton peak E_{1h} is missing and the dip in the polarization at the peak labelled $E_{1\ell}$ shows it is of light hole character.

temperature is increased, holes can boil out of the bottom of the valence band and hence allow the formation of the correlated electron–hole pairs required for E_{1h} excitons. However, it has not been demonstrated theoretically that the Pauli exclusion principle should come into play at smaller hole densities than that required for significant screening of the excitons.

4.2. n-type modulation and antimodulation doped quantum wells

Prior to the investigation of n-type modulation-doped structures, n-type antimodulation doped GaAs quantum wells were investigated to compliment earlier studies on p-type antimodulation doped wells [10,18]. In the antimodulation doped configuration, the impurity is restricted to the quantum well during growth. Most striking with these n-type structures was the observation that with increasing n-type doping (Si), the circular polarization of the luminescence at 5 K with resonant excitation of the $n=2$ heavy hole exciton decreases markedly and, in fact, becomes opposite to that of the excitation for [Si] $\approx 10^{18}$ cm^{-3} [23].

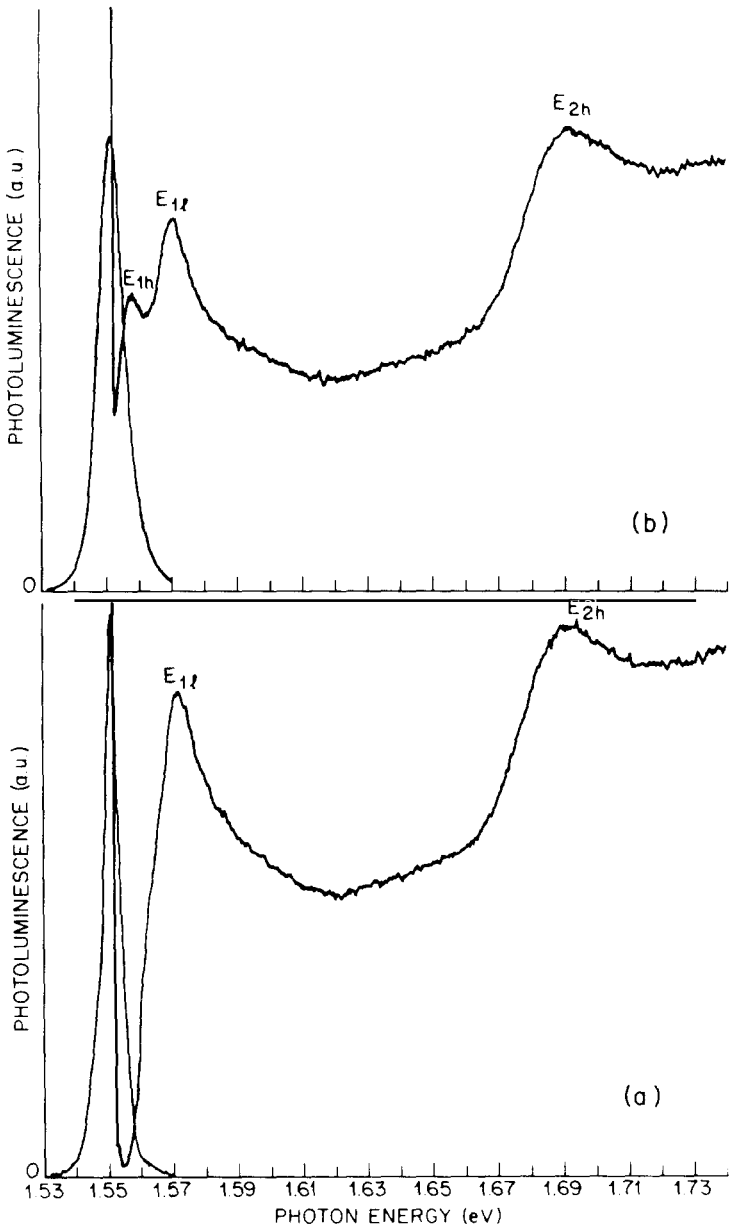

Fig. 7. Photoluminescence and excitation spectra at 5 K (a) and 43 K (b) for the same sample described in connection with fig. 6. At 43 K, a distinct peak due to E_{1h} can be seen. The emission is Stokes shifted from this peak by $\cong 6.5$ meV.

Furthermore, in spite of the large background of unpolarized electrons, the Si-doped quantum wells can exhibit highly polarized luminescence, especially for resonant excitation of E_{1h}. These anomalous characteristics of the polarization were greatly reduced, or even absent, when the sample temperature was increased to ≈ 20 K. At the same time, the polarization of the extrinsic luminescence at energies lower than that of the main peak is not anomalous and shows relatively small changes in magnitude over the 5–20 K temperature range. The mechanism that can result in a negative polarization for resonant excitation of E_{2h} in the Si-doped GaAs wells would seem to require a spin flip of the optically excited electrons and/or holes, or excitons, that give rise to the main luminescence peak. Such a mechanism has not been proposed.

Subsequently, n-type modulation doped GaAs quantum wells were investigated. One such structure incorporated 20 periods of $L = 104$ Å GaAs well and 227 Å thick superlattice barriers doped in the center 24 Å with Si to give $N_e = 1.4 \times 10^{11}$ cm^{-2}. The photoluminescence for this sample shown in fig. 8 exhibits all the anomalous characteristics mentioned above for the Si antimodulation doped structures and hence suggests that it is the electron gas which gives rise to the negative polarization effect. Although this would seem to be a simpler

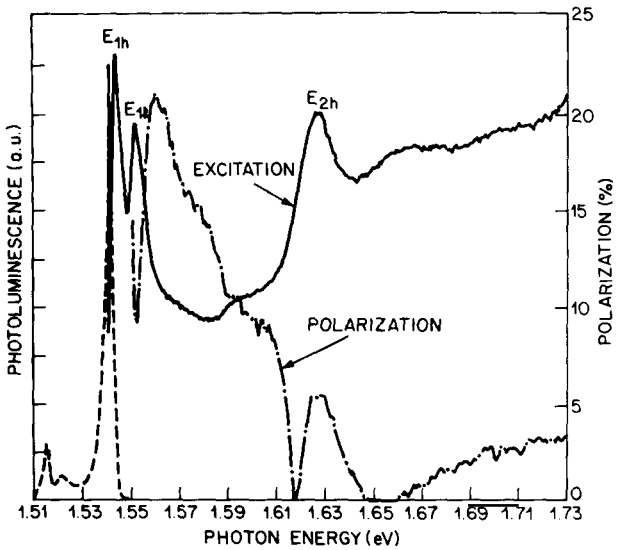

Fig. 8. Photoluminescence (dashed), excitation (solid), and polarization (dashed-dotted) spectra at 5 K for an n-type modulation doped GaAs quantum well sample $L = 104$ Å and superlattice barriers $x \approx 0.3$, doped in the center 24 Å with Si to give $N_e = 1.4 \times 10^{11}$ cm^{-2}. The phase of the detected polarization signal has been changed by 180° between $E_p \cong 1.617$ eV and 1.652 eV so that the polarization detected is actually negative for excitation between these two energies, i.e., for resonant excitation of E_{2h}.

system to investigate from a theoretical point of view than the Si-doped wells, a viable mechanism has yet to be proposed.

The excitation spectra of the GaAs wells doped with electrons or Si donors exhibit some of the same characteristics as p-type modulation doped GaAs wells. In particular, one observes a broadening and weakening of E_{1i} relative to E_{2h}, the gradual rise in the luminescence level as E_p approaches $E_{1\ell}$ from above, and a Stokes shift between emission and absorption (excitation). Although some data suggest that E_{1h} is affected more than $E_{1\ell}$ in the electron containing GaAs wells, the effects are not nearly as pronounced as those for holes in the wells as discussed above. In contrast to the p-type quantum wells, with $N_e \cong 5 \times 10^{11}$ cm^{-2}, there is no evidence of E_{1i} and perhaps other low lying exciton transitions [24]. However there is a weak modulation, $\approx 15\%$, on the excitation spectrum for higher quantum number transitions indicating weakened electron–hole final state interactions, presumably due to screening.

4.3. Stokes shifts

It has been noted that Stokes shifts between emission and absorption are observed for the modulation doped GaAs quantum wells. Attempts to explain the size of the Stokes shifts with a simple model which assumes equal exciton contributions in absorption and emission have not met with success. This model also includes; effects that arise from the electrostatic potential (band bending) due to the charge transfer from the alloy to the quantum well [21], calculations of the resultant electron and hole energy levels, and computations of the Fermi level. As an example of the failure of this simple model, for electron and hole densities in the range $1\ 2 \times 10^{11}$ cm^{-2}, the observed Stokes shifts are significantly smaller than that predicted by the simple model, typically by about 5 meV. These results may be indicating that exciton effects are significantly less in emission than in absorption. There are also some difficulties with the sample parameters although it appears that this cannot be the only problem.

5. Fitting GaAs quantum well exciton transitions – energy gap discontinuties

Dingle et al. [4] were quite successful in fitting the series of exciton transitions for GaAs quantum wells as observed in absorption. The parameters used in this early work have by and large been accepted until very recently. Of most importance is the division of the energy-gap discontinuity $\Delta E_g = E_g(\text{AlGaAs}) - E_g(\text{GaAs})$ between the conduction and valence band wells. It was concluded that the $\Delta n = 0$ allowed transitions could be fit with a conduction band offset, $\Delta E_c = Q_e \Delta E_g$, with $Q_e = 0.85 \pm 0.03$ which then leads to a valence band offset $\Delta E_v = Q_h \Delta E_g = (1 - Q_e)\Delta E_g$ with $Q_h = 0.15 \pm 0.03$. The effective masses employed were; $m_e^* = 0.0665 m_o$, $m_h^* = 0.45 m_o$, and $m_l^* = 0.080 m_o$. Dingle et al. did

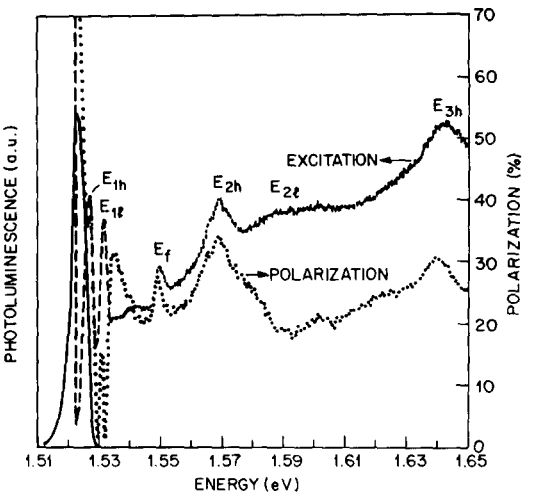

Fig. 9. Photoluminescence (dashed), excitation (solid), and polarization (dotted) spectra at 5 K for an undoped GaAs multiquantum well sample with $L = 180$ Å wells and 211 Å $x = 0.29$ alloy barriers. The phase of the polarization has been changed by 180 Å for excitation at $E_p = 1.53$ eV to show the negative polarization due to $E_{1\ell}$. For E_p equal to the energy of the forbidden transition E_f, a distinct increase in polarization shows this transition is of heavy hole character leading to the assignment $E_{1\,3h}$.

not claim to fit the forbidden exciton transitions which appeared in the data. Polarization measurements [5], including the data in fig. 9, show that this forbidden transition is heavy hole in character so that it has been assigned to the $\Delta n = 2$ parity allowed exciton involving the $n = 1$ electron and the $n = 3$ heavy hole, i.e., $E_{1\,3h}$. For GaAs wells with $L = 100$ Å and $x = 0.3$ alloy barriers, the calculated (above or "usual" parameters) and observed $E_{1\,3h}$ exciton transitions energies measured from the E_{1h} peak are 38 meV and 64 meV, respectively. This serious discrepancy has been known for some time but has not emphasized [4].

5.1. Parabolic GaAs quantum wells

GaAs quantum wells with a parabolic potential profile have been grown by MBE and their photoluminescence properties investigated at low temperatures [25]. Parabolic potential wells are of special interest since the Q's appear directly in the eigenvalue expressions. For square wells with infinite barriers

$$E_{ni} = (1/2m_i^*)[n\pi\hbar/L_z]^2, \tag{1}$$

where $n = 1, 2, 3$, etc. With parabolic wells

$$E_{ni} = (n - 1/2)\hbar\omega_{0i}, \tag{2}$$

where again $n=1,2,3$, etc. and $\omega_{0i}=\sqrt{K_i/m_i^*}$ with K_i equal to the curvature of the parabolic well. Defining K_i by the potential height of the finite parabolic well with $z=\pm L/2$, namely, $Q_i\Delta E_g$, one has

$$E_{ni}=2(n-1/2)\frac{\hbar}{L}\left[\frac{2Q_i\Delta E_g}{m_i^*}\right]^{1/2}. \tag{3}$$

Parabolic profiles of aluminum content were generated by chopping an aluminum molecular beam with a computer controlled shutter. The duty ratio during which the aluminum beam was turned on was made proportional to the desired concentration and potential profile, reaching unity for the barriers. Each well consisted of 41 layers. Three samples were grown by this technique.

Photoluminescence measurements at 5 K shown in fig. 10 reflect the expected harmonic oscillator like electron and hole energy levels. Analyses of the energies of the various exciton transitions and their polarization characteristics lead to their identification. Differences in the energies of these transitions are then used to determine the electron, heavy hole, and light hole energy level ladders, ΔE_e, ΔE_h, and ΔE_ℓ, respectively. For these estimates, the binding energies of all the excitons were assumed equal.

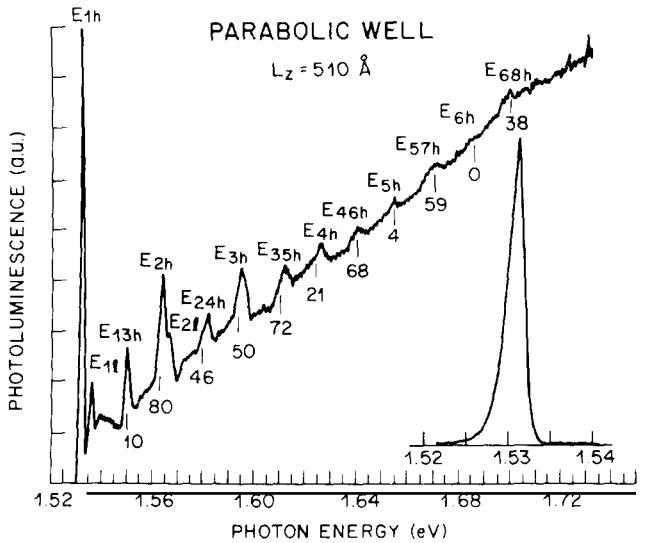

Fig. 10. Photoluminescence (insert) and excitation spectra at 5 K for GaAs quantum wells with a parabolic profile. The wells were of width $L=510\pm35$ Å measured at the 225 Å wide $x=0.30\pm0.06$ alloy barriers. Short vertical bars show the calculated energies of the various heavy hole exciton transitions with $Q_e=0.51$ and the usual effective masses. The integers below the peaks represent the calculated strengths normalized to 100 for E_{1h} (without the resonant enhancement) and demonstrate, in agreement with the data, that the $\Delta n=2$ transitions gain strength relative to the $\Delta n=0$ transitions as n increases.

The agreement between these experimental ΔE_i and those calculated from eq. (3) was very poor. Removing the L dependence by taking ratios gives, for example, $\Delta E_e/\Delta E_h = 2.6$ for the experimental value to be compared with the calculated value

$$[Q_e m_h^*/(1-Q_e)m_e^*]^{1/2} = 6.0, \tag{4}$$

using the usual parameters. This discrepancy is not significantly improved using an exact calculation for E_{ni} which takes into account finite barrier heights and the variation of the effective mass with z. With the usual effective masses, eq. (4) requires that $Q_e \approx 0.5$ to fit the experimental ratio 2.6, in marked contrast to the usual value of 0.85 [1,4]. The many allowed and forbidden heavy hole transitions observed with the parabolic well samples can be fit accurately with $Q_e \approx Q_h$ using the usual effective masses as shown in fig. 10. However, $Q_e \approx 0.5$ with the m_i^* cited above does not lead to satisfactory fits of observed series of exciton transitions for square wells, and conversely, $Q_e = 0.85$ does not lead to acceptable fits of the parabolic well data.

5.1. Unified picture

It is clear that what is needed to fit the square well forbidden transitions is a smaller heavy hole mass and/or a larger Q_h than usually assumed. As a result, a heavy hole mass of $0.34m_0$ has been proposed for these quantum well structures [26]. This value is consistent with that utilized in some theoretical work [27,28] and also obtained by Kleinman in some earlier attempts to fit square quantum well data for wide wells [15]. With this m_h^* and the usual m_e^*, $Q_e \approx 0.57$ is required to fit the parabolic well $\Delta E_e/\Delta E_h$ data via eq. (4). Similar arguments with $Q_e = 0.57$ for the light hole transitions for parabolic wells requires that $m_l^* = 0.94m_0$ which is about 7% larger than the value ($0.088m_0$) preferred earlier for square wells. Thus the new parameters proposed [26] for both parabolic and square wells are; $Q_e = 0.57$, $m_e^* = 0.0665m_0$, $m_h^* = 0.34m_0$, and $m_l^* = 0.094m_0$.

The energies of the various light and heavy hole exciton transitions have been calculated with these new parameters as a function of L for square wells. As shown in fig. 11 these calculated energies are found to be in good agreement with the corresponding experimental energies including those for the forbidden transitions determined from excitation spectra for ten different high-quality multiquantum square well samples grown by MBE with L ranging from 51 Å to 521 Å and alloy barriers with $x \cong 0.3$.

The new parameters have been obtained in such a manner that the ratios involving the ΔE_i for the parabolic wells agree with the parabolic well data. However the values of L required via eq. (3), or the exact calculation, for the calculated ΔE_i to agree with the data using the new parameters are in agreement with the values of L estimated from the growth parameters. This is the case for all three parabolic well samples [26].

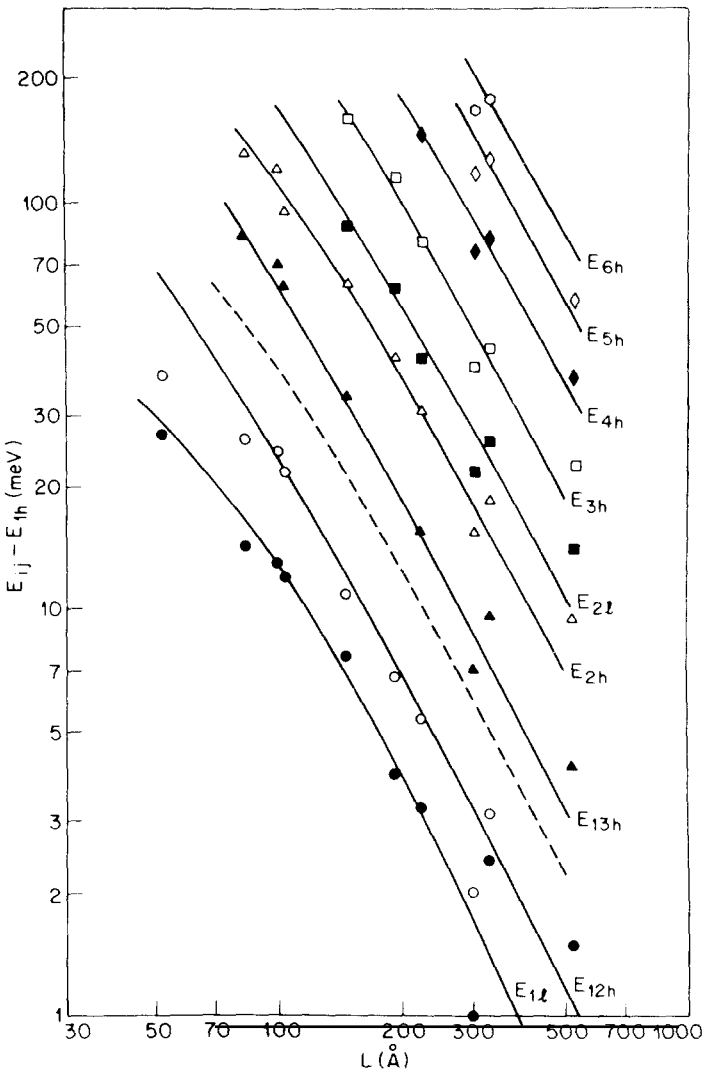

Fig. 11. Logarithm of the observed energies of the exciton transitions E_{ij} measured from the $n=1$ heavy hole exciton E_{1h} versus the logarithm of L for a series of high-quality square GaAs multi-quantum well samples with $x=0.30\pm0.05$ alloy barriers. The solid lines are the calculated E_{ij} E_{1h} using the new parameters: $Q_c=0.57$, $m_e^*/m_0=0.0665$, $m_h^*/m_0=0.34$, and $m_\ell^*/m_0=0.094$. The dashed line represents E_{13h} E_{1h} calculated with the usual parameters, $Q_c=0.85$ and $m_h^*/m_0=0.45$.

The calculations discussed above do not include effects due to the non-parabolicity (NP) of the conduction and light hole bands. For the heavy hole, NP is negligible. The effects of NP on the eigenvalues for both square and parabolic wells have been estimated and are found to be of order 7% for the

highest energies and hence nontrivial, but generally too small compared to other uncertainties to effect significantly the comparison between theory and experiment [26].

Thus a single set of parameters leads to acceptable fits to the observed exciton transitions for both square and parabolic potential wells. A fine tuning of these parameters could lead to slightly different Q values, but the extensive data cited herein, and other data of a different nature not cited, lend strong support to $Q_e \approx 0.6$ in contrast to the previously accepted value $Q_e \approx 0.85$. These results emphasize the importance of the forbidden exciton transitions and the parabolic quantum wells for determining the GaAs quantum well parameters.

6. Acknowledgements

The authors wish to acknowledge the most important contributions of R.D. Dupuis, A.C. Gossard, Won T. Tsang and W. Wiegmann in providing the many unique structures whose properties have been discussed herein. In addition, the data acquisition and manipulation skills of O. Munteanu greatly facilitated the accumulation of the recent results presented.

References

[1] R. Dingle, W. Wiegmann and C.H. Henry, Phys. Rev. Lett. 33 (1974) 827.
[2] R. Dingle, C. Weisbuch, H.L. Stormer, H. Morkoc and A.Y. Cho, Appl. Phys. Lett. 40 (1982 507.
[3] C. Weisbuch, R.C. Miller, R. Dingle, A.C. Gossard and W. Wiegmann, Solid State Commun. 37 (1981) 219.
[4] R. Dingle, Festkorperprobleme 15 (1975) 21.
[5] R.C. Miller, D.A. Kleinman, W.A. Nordland, Jr. and A.C. Gossard, Phys. Rev. B22 (1980) 863.
[6] See, for example, G. Lampel, Proc. XIIth Int. Conf. Physics of Semiconductors, Stuttgart, 1974, ed., M.H. Pilkuhn (Teubner, Stuttgart, 1974) p. 743.
[7] Q.H.F. Vrehen, J. Phys. Chem. Solids 29 (1968) 129.
[8] A. L. Mears and R.A. Stradling, J. Phys. C 4 (1971) L22.
[9] B.P. Zakharchenya, V.I. Zemskii and D.N. Mirlin, Zh. Eksp, Teor. Fiz. 70 (1976) 1092 [Sov. Phys. JETP 43 (1976) 569].
[10] R.C. Miller, A.C. Gossard and W.T. Tsang, Physica 117B and 118B (1983) 714.
[11] R.C. Miller, D.A. Kleinman, W.T. Tsang and A.C. Gossard, Phys. Rev. B 24 (1981) 1134.
[12] G. Bastard, E.E. Mendez, L.L. Chang and L. Esaki, Phys. Rev. B 26 (1982) 1974.
[13] R.L. Greene, K.K. Bajaj and D.E. Phelps, Phys. Rev. B 29 (1984) 1807.
[14] R.C. Miller, D.A. Kleinman, A.C. Gossard and O. Munteanu, Phys. Rev. B 25 (1982) 6545.
[15] D.A. Kleinman, Phys. Rev. B 28 (1983) 871.
[16] W.F. Brinkman, T.M. Rice, and B. Bell, Phys. Rev. B 8 (1973) 1570.
[17] J.R. Haynes, Phys. Rev. Lett 4 (1960) 361.
[18] R.C. Miller, A.C. Gossard, W.T. Tsang and O. Munteanu, Solid State Commun. 43 (1982) 7, 519.
[19] J. Hegarty, M.D. Sturge, C. Weisbuch, A.C. Gossard and W. Wiegmann, Phys. Rev. Lett. 49 (1982) 930.

[20] R. C. Miller, R.D. Dupuis and P.M. Petroff, Appl. Phys. Lett. 44 (1984) 508.
[21] R. Dingle, H.L. Stormer, A.C. Gossard and W. Wiegmann, Appl. Phys. Lett. 33 (1978) 665.
[22] D.A. Kleinman (unpublished).
[23] R.C. Miller and A.C. Gossard, Phys. Rev. B 28 (1983) 3645.
[24] A. Pinczuk, J. Shah, R.C. Miller, A.C. Gossard, and W. Wiegmann, Solid State Commun. 50 (1984) 735.
[25] R.C. Miller, A.C. Gossard, D.A. Kleinman and O. Munteanu, Phys. Rev. B 29 (1984) 3740.
[26] R.C. Miller, D.A. Kleinman and A.C. Gossard, Phys. Rev. B 29 (1984) 7085.
[27] P. Lawaetz, Phys. Rev. B 4 (1971) 3460.
[28] A. Baldereschi and N.O. Lipari, Phys. Rev. B 3 (1971) 439.